

On Channel State Feedback Model and Overhead in Theoretical and Practical Views

Chunbo Luo, University of Exeter, c.luo@exeter.ac.uk

Abstract—Channel state feedback plays an important role to the improvement of link performance in current wireless communication systems, and even more in the next generation. The feedback information, however, consumes the uplink bandwidth and thus generates overhead. In this paper, we investigate the impact of channel state feedback and propose an improved scheme to reduce the overhead in practical communication systems. Compared with existing schemes, we introduce a more accurate channel model to describe practical wireless channels and obtain the theoretical lower bounds of overhead for the periodical and aperiodical feedback schemes. The obtained theoretical results provide us the guidance to optimise the design of feedback systems, such as the number of bits used for quantizing channel states. We thus propose a practical feedback scheme that achieves low overhead and improved performance over currently widely used schemes such as zero holding. Simulation experiments confirm its advantages and suggest its potentially wide applications in the next generation of wireless systems.

Index Terms—Channel state feedback, CSI, channel modelling, periodical feedback, aperiodical feedback, zero holding

I. INTRODUCTION

One of the key technologies in 4G communication systems is channel state information (CSI) feedback, which is gaining increased importance in the research and design of 5G systems that are undergoing the standardization stage. The importance will be even significant in 6G which includes communication and satellite positioning system [1]–[4]. The importance of CSI feedback can be simply summarized as that more knowledge of the wireless channel can enhance the system’s throughput. Such advantage is achieved through novel schemes including precoding, modulation and coding scheme (MCS) selection, or beam selection. As an essential technology for the 5G systems, millimeter wave provides exceptionally high throughput, but also comes with the down sides such as reflection, scattering, and blockage, which cause more frequent change of channel states since its wave length is shorter than traditional wireless carriers. Therefore, the feedback of CSI needs to be more frequent than current cellular systems in order to maintain a high throughput link. The increased feedback data would generate a lot of overhead and consume excessive bandwidth that is essential for other types of services in 5G systems. To optimize the feedback overhead is thus a key research topic for improving spectrum resource, which motivates this paper.

The benefits of CSI feedback have been recognized for long time and exploited in contemporary wireless systems. We will briefly introduce several recently reported examples. In [5], [6], the channel states sent back to a transmitter are used for precoding. In [7], [8], authors proposed novel interference analysis and cancellation schemes driven by the channel states

feedback information. Authors of [9], [10] studied the benefits of CSI feedback for optimizing resource allocation. In addition to these benefits, pioneering studies on physical layer security have showed the power of CSI feedback on the improvement of communication security [11], [12].

The benefits of CSI feedback come with the cost of increased overhead that consumes the uplink spectrum resource. For the purpose of reducing this cost, optimization schemes have been widely studied. In [13], [14], compressed sensing (CS) is leveraged to reduce the number of the bits for CSI feedback. Two issues are in association with the CS based method. First, the delay is significantly large since CS is a blockwise signal processing method and is usually solved via a large number of iterative calculation. Second, CS relies on the presumption of the downlink channel being sparse. Such a sparsity assumption has not been fully investigated in research. As a more matured method, a discrete cosine transform (DCT) basis matrix is designed to compress the channel states in [15]. DCT is a blockwise signal processing method, and the efficiency is proportionally related to the length of the data blocks for DCT. Therefore, there exists a trade-off between the compression efficiency and timeliness of CSI feedback.

As shown in the generation of fading channels [16]–[18], fading channel is indeed a stationary random process which allows us to predict a channel state based on its previous several observations. This model is also used in the estimation of the channel state information [19]. The difference of a prediction versus its real channel state is usually called as the innovation of a channel. For a stationary fading channel, the feedback of innovation can be utilized to reconstruct full channel states. Generally, the quantization of the innovation needs less bits than the quantization of original channel. Therefore, the feedback of quantized innovation is also recognized as an effective CSI feedback technology. In literature, the quantization and feedback of channel innovation are usually called as differential channel state feedback methods.

The order-one autoregressive (AR) model is often used to model a fading channel [20], [21]. Based on the AR(1) model, the difference between a channel state x_k and \hat{x}_k , where the latter is the prediction of x_k based on x_{k-1} , is quantized. In such a differential feedback scheme, the minimum number of bits, known as feedback overhead, is estimated. Similar to the method in [20], AR(1) model based differential quantization is also investigated in [21]. Different from the scalar quantization in [20], vector quantization is considered in [21], which claims that vector quantization has advantages over the scalar one. On the transmission of CSI feedback, several methods have

been proposed. In [22], there is no feedback loop at the CSI transmitter side, and quantization noise will be accumulated when the channel state is reconstructed at the receiver side. The same problem also exists in the method proposed in [23]. Different from the work in [22], rate distortion theory is employed to estimate the lower bound of the quantization bits under the constraint of channel reconstruction mean square error (MSE) [23]. However, we can deduce that the rate distortion function calculated in [23] does not have the right distortion when the number of quantization bits is zero.

Based on the introduction above, there are basically two types of CSI feedback schemes. The first type focuses on the feedback of original channel states [13]–[15], and the second one is based on the transmission of differential channel states [20]–[25]. The latter ones are gaining more popularity because of their ability to reduce redundancy between adjacent channel states [26], and thus require less data bits than the schemes that transmit the original channel states. However, existing differential feedback schemes are of problems regarding the following three aspects. First, the channel modelling is not accurate. In literature, the order one autoregressive structure such as the AR(1) model is widely used to describe a fading channel, and is not accurate description of Rayleigh or Rician channels. Furthermore, channel fading and additive noise are not simultaneously considered in literature, i.e., the additive white Gaussian noise (AWGN) is not taken into account at the modelling of channel fading. Third, open loop differential schemes are considered in literature, but they have the high risk of accumulating quantization noise. A closed loop structure is necessary to correct the channel distortion in time and avoid noise accumulation.

In this paper, we consider fading channels to be the response of white Gaussian variables passing through an autoregressive structure. Different from the AR(1) model, the order of the autoregressive structure is not assumed to be in rank one, rather a more realistic setting greater than one and extensible to infinitely large. Besides, AWGN is simultaneously considered with channel fading in our analysis. Based on the more complete channel model, we first investigate the effect of operation delay on the overhead. To reduce the accuracy degradation caused by delay, we predict the channel state given its previous a few observations. Since the prediction has intrinsic finite accuracy, we use the channel state mean square error (MSE) to investigate the accuracy, which is essentially equal to the channel reconstruction distortion in the extreme case of infinite-bits feedback. Afterwards, we obtain the theoretic lower bound of MSE given finite-bits of CSI feedback. Both periodical and aperiodical feedback schemes adopted by standards are analysed using the rate distortion theory. Under the guidance of theoretic results, we propose a novel and practical CSI feedback method based on more realistic channel modelling and parameter configuration, which achieves improved long-term performance over contemporary methods, confirmed by both theoretical study and extensive experiments.

The rate distortion theory based feedback overhead optimization is also performed in [27] where the theoretic work is performed. We pay more attention to finding a practical solu-

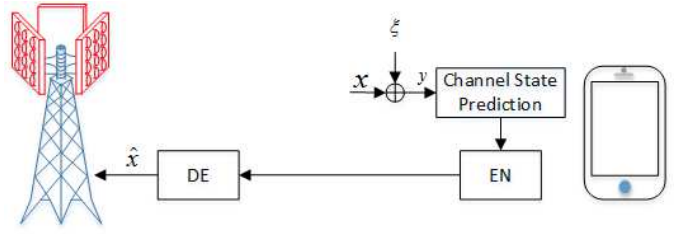


Fig. 1. System diagram.

tion to optimizing feedback overhead. The network overhead for compressed sensing is estimated in [18], [28]–[30].

The rest of this paper is organized as follows. Introduction to traditional channel feedback systems and problem formulation are presented in Section II. In Section III, we analyze the minimum MSE of the extreme case of infinite bits used for channel state feedback, and compare our results with that of channel estimation based on the zero-holding rule. The rate distortion theory is employed to calculate the theoretic lower bounds on bits for both aperiodical and periodical feedback schemes in IV. We propose a novel channel state feedback scheme with performance analysis in Section V. Numerical simulations are performed in Section VI followed by conclusions in Section VII.

II. PROBLEM FORMULATION

The channel state feedback scheme is shown in Fig. 1. The fading channel is denoted by x . Let x_k denote the channel sample at the k -th time instance. The fading channel state is not accessible due to the AWGN which is denoted by ξ . The additive noise at the k -th time instance is ξ_k . The overall degraded channel, accessible from the measurements of the reference signals, can be denoted as follows,

$$y_k = x_k + \xi_k. \quad (1)$$

The widely adopted Rayleigh channel model is also used in our analysis, which can be extended to other channel models following a similar method. According to the definition of Rayleigh distribution, both the In-phase and Quadrature component of x follow a Gaussian distribution. It is easy to know that a Gaussian random process is the response of a white Gaussian variable passing through an AR structure that determines the spectrum of the random process. Let ψ_k denote this variable, and x_k can be modelled as follows

$$x_k = \sum_{m=1}^L a_m x_{k-m} + \psi_k, \quad (2)$$

where ψ_k is a variable following the Gaussian distribution with mean zero and variance of σ_ψ^2 , and L is the memory depth of the random process equal to the order of the AR structure.

Due to the protocol stack and signal processing procedure, there inevitably exists operation delay in a feedback system. To counteract the accuracy degradation caused by delays, a series of noisy observations of the fading channel are used to obtain one-step forward predictions of the channel state. Without loss of generality, the noisy observations are represented by $Y_{k,1:L} = (y_{k-L+1}, y_{k-L+2}, \dots, y_k)^T$.

With the predicted channel state or the channel innovation, the user equipment (UE) will encode and send it to the base station. The transmission of the codewords consumes the uplink bandwidth. To quantitatively evaluate the performance of a feedback system, we calculate the average bit rate R required for sending through the codewords. Details about R and the encoding procedure will be introduced in the following sections. At the base station, the codewords are decoded to reconstruct the fading channel, denoted by \hat{x}_{k+1} .

As in the introduction of the system model, only the noisy observation of channel y can be directly read, rather than the original channel state x . R is thus related to y . Different concrete quantization methods generate different size of R . To remove the limits brought in by concrete methods, the mutual information between y and \hat{x} is taken as the metric to express R . Essentially, the mutual information is a theoretical lower bound on R which is written as follows,

$$I(y_{k+1}; \hat{x}_{k+1}). \quad (3)$$

Furthermore, we can straightforwardly investigate the trade-off between R and the channel reconstruction accuracy. Generally, higher accuracy requires more bits for quantization. The accuracy is measured by MSE between the real channel state x_{k+1} and its reconstruction \hat{x}_{k+1} , which is defined as follows,

$$D_x = E \left[(x_{k+1} - \hat{x}_{k+1})^2 \right], \quad (4)$$

where $E[\cdot]$ denotes the expectation.

We can now formulate the optimization problem that aims to minimize the number of bits under the constraint of channel reconstruction MSE,

$$\begin{cases} \text{Objective : } R = \inf \left\{ \frac{1}{L} I(y_{k,1:L}; \hat{x}_{k+1}) \right\} \\ \text{subject to : } d(x_{k+1}, \hat{x}_{k+1}) \leq D_x \end{cases}. \quad (5)$$

For the purpose of analysis, we introduce an auxiliary variable \hat{y}_{k+1} . The physical sense of \hat{y}_{k+1} is regarded as the reconstructed y_{k+1} . The relationship between \hat{y}_{k+1} and \hat{x}_{k+1} is defined as follows,

$$\hat{x}_{k+1} \triangleq \frac{\sigma_x^2}{\sigma_x^2 + \sigma_\xi^2} \hat{y}_{k+1}. \quad (6)$$

Since \hat{x}_{k+1} is the scaled \hat{y}_{k+1} by a constant, the following two definitions of mutual information are equal to each other: $\frac{1}{L} I(y_{k,1:L}; \hat{x}_{k+1}) = \frac{1}{L} I(y_{k,1:L}; \hat{y}_{k+1})$. The optimization problem defined in (5) is thus converted to the following form:

$$\begin{cases} \text{Objective : } R = \inf \left\{ \frac{1}{L} I(y_{k,1:L}; \hat{y}_{k,1:L}) \right\} \\ \text{subject to : } d(x_{k+1}, \hat{x}_{k+1}) \leq D_x \end{cases}. \quad (7)$$

As designed in the 3GPP standards, channel states can be sent back to the base station periodically or aperiodically. The differences between these two methods have fundamental impact towards the solution of (7). The following sections will investigate both cases in order to find the optimal feedback schemes under the constraint of MSE.

III. AN EXTREME CASE: INFINITE BITS FEEDBACK AND RECONSTRUCTION MSE

The previous section introduces two metrics to evaluate a channel state feedback scheme: channel reconstruction accu-

racy and the number of bits. In this section, we consider that channel states are sent to BS in real numbers, which can only be achieved by representing a channel state with infinite bits. The work in this section thus reveals the reconstruction distortion D_x at the extreme case of $R \rightarrow \infty$.

In literature, the channel state observed at the current time instance is usually adopted as the state at the next time instance. Such a channel state determination strategy is called *zero-holding* (ZH). We will compare the MSE of the reconstructed channel states from the ZH strategy and that from our prediction method.

A. MMSE in one-step ahead prediction based on real-valued channel states feedback

Since infinite large number of bits are used to quantize the channel state feedback, there will be no quantization loss. The channel reconstruction accuracy is fully determined by the error occurring in the one-step ahead prediction of x_{k+1} given $y_{k,1:L}$. Thus, the lower bound on the distortion D_x at $R \rightarrow \infty$ is equal to the MMSE of x_{k+1} ,

$$D_x|_{R \rightarrow \infty} = E \left[(x_{k+1} - x'_{k+1})^2 \right], \quad (8)$$

where x'_{k+1} is the MMSE prediction of x_{k+1} given the real-valued channel states feedback, that is,

$$x'_{k+1} = E[x_{k+1}|y_{k,1:L}]. \quad (9)$$

Since y_k , $k \in \mathbb{Z}$, is the noisy observation of x_k under additive Gaussian noise ξ_k , the MMSE estimation of x_k given y_k is in a linear form. Furthermore, we can easily prove that y is a spherical invariant random process. Thus, there exists a linear extrapolation of y_{k+1} based on $y_{k,1:L}$. Furthermore, we know that there exists a MMSE linear prediction of x_{k+1} given $y_{k,1:L}$. Let Θ denote the coefficients of the linear predictor. Based on the results in [31], the coefficient vector Θ of the MMSE predictor is calculated by

$$\Theta = \begin{bmatrix} \kappa_{xy}(1) \\ \kappa_{xy}(2) \\ \vdots \\ \kappa_{xy}(L) \end{bmatrix}^T \mathbf{K} \quad (10)$$

where $\kappa_{xy}(i) = E[x_{k+1}y_{k+1-i}]$, $l \in \mathcal{L}$ and $\mathcal{L} = \{1, 2, \dots, L\}$ and

$$\mathbf{K} = \begin{bmatrix} \kappa_y(0) & \kappa_y(1) & \dots & \kappa_y(L-1) \\ \kappa_y(1) & \kappa_y(0) & \dots & \kappa_y(L-2) \\ \vdots & \vdots & \ddots & \vdots \\ \kappa_y(L-1) & \kappa_y(L-2) & \dots & \kappa_y(0) \end{bmatrix}. \quad (11)$$

With the defined order- L coefficients Θ , the MMSE prediction of x_{k+1} given $y_{k,1:L}$ is calculated as follows,

$$x'_{k+1} = \Theta \cdot \begin{bmatrix} y_{k-L+1} \\ y_{k-L+2} \\ \vdots \\ y_k \end{bmatrix}. \quad (12)$$

According to the results in [31], the mean square error in

real-valued channel state feedback $D_x|_{R \rightarrow \infty}$ is calculated via

$$D_x|_{R \rightarrow \infty} = \sigma_x^2 - \begin{bmatrix} \kappa_{xy}(1) \\ \kappa_{xy}(2) \\ \vdots \\ \kappa_{xy}(L) \end{bmatrix}' \cdot \mathbf{K}^{-1} \cdot \begin{bmatrix} \kappa_{xy}(1) \\ \kappa_{xy}(2) \\ \vdots \\ \kappa_{xy}(L) \end{bmatrix} \quad (13)$$

$$\triangleq \sigma_P^2.$$

The distortion of the reconstructed channel based on one-step ahead prediction has been obtained for the extreme case of $R \rightarrow \infty$. Next, the distortion for ZH strategy will be calculated.

B. MMSE in zero-holding channel state determination

In the literature, not much attention has been paid on the operation delay of channel state feedback. The current channel state is taken as the one at the next time instance which is called as zero-holding. In this subsection, we will quantitatively determine the distortion occurring in the zero-holding strategy as a contrast to the one-step ahead prediction strategy. Let \hat{x}_{k+1}^Z denote the channel state at $(k+1)$ -th time instance determined via the ZH rule. The ZH strategy can be mathematically described as follows,

$$\hat{x}_{k+1}^Z = x_k^\dagger, \quad (14)$$

where x_k^\dagger denotes the estimation of x_k .

The MMSE estimation of current channel state is an optimum estimation given additive Gaussian noise, which is widely used in literature. Since x_k^\dagger is the MMSE estimation of x_k given y_k , we have the following equation,

$$x_k^\dagger = E[x_k|y_k]. \quad (15)$$

Channel distortion is similarly measured by the MSE of the reconstructed channel x^\dagger versus its real value x as follows,

$$\begin{aligned} \sigma_Z^2 &= E[(x_{k+1} - \hat{x}_{k+1}^Z)^2] = E[(x_{k+1} - x_k^\dagger)^2] \\ &= E[(x_{k+1} - x_k - (x_k - x_k^\dagger))^2] \\ &= E[(x_{k+1}^2)] + E[(x_k^2)] + E[(x_k - x_k^\dagger)^2] \\ &\quad - 2E[(x_{k+1}x_k)] - 2E[(x_{k+1}(x_k - x_k^\dagger))] \\ &\quad + 2E[(x_k(x_k - x_k^\dagger))] \\ &\stackrel{(a)}{=} 2\sigma_x^2 - 2\kappa_x(1) + \frac{\sigma_x^2\sigma_\xi^2}{\sigma_x^2 + \sigma_\xi^2}, \end{aligned} \quad (16)$$

where σ_Z^2 denotes the MSE, and in (a), the first two terms are calculated as follows

$$\begin{aligned} E[(x_{k+1}^2)] &= E[(x_k^2)] = \sigma_x^2 \\ E[(x_{k+1}x_k)] &= \kappa_x(1) \end{aligned} \quad (17)$$

following the definition of autocorrelation of a random process. The third term in (a) is calculated as follows

$$E[(x_k - x_k^\dagger)^2] = \frac{\sigma_x^2\sigma_\xi^2}{\sigma_x^2 + \sigma_\xi^2}, \quad (18)$$

where the orthogonal principle has been employed,

$$E[(x_k(x_k - x_k^\dagger))] = E[(x_{k+1}(x_k - x_k^\dagger))] = 0. \quad (19)$$

We have obtained the channel reconstruction distortion for both the one-step ahead prediction scheme and ZH strategy. The results are obtained at the extreme case that infinite number of bits are used to quantize the channel state. Next, we will investigate a more practical case that only finite bits are used to convey the channel states from a UE to a base station.

IV. THEORETIC LOWER BOUNDS ON FINITE-BITS REPRESENTED CHANNEL STATES FEEDBACK

As mentioned in Section II, the two types of channel state feedback schemes in 3GPP LTE, aperiodic and periodic feedback transmission, are also considered in the next generation of cellular systems (5G). It is thus significantly important to know the theoretical lower bounds of the length of bits required by these two schemes.

A. An Overhead Lower Bound in Aperiodic Feedback

The aperiodic feedback scheme works in such a protocol that a base station sends a request of downlink channel states when needed, and then the UE sends the channel state information back to the base station, which is unavoidably delayed due to the protocol stack and signal processing. This reactive style implies that the time interval between two channel state transmissions keeps changing. Since the feedback intervals vary, the vector quantization does not fit for compressing the channel states. Therefore, channel states are quantized via sample-wise quantization, and sent back to the base station. We can thus obtain the lower bound of the scalar quantization method, which is related to the entropy of a single channel sample as follows.

1) *Aperiodic feedback of one-step ahead predicted channel state*: The direct solution to (7) can hardly be achieved. Before calculating the theoretic lower bound, we define an auxiliary variable d_y , the MSE between $y_{k,1:L}$ and $\hat{y}_{k,1:L}$, as follows,

$$d_y = \sum_{l=1}^L E[\theta_l^2 (y_{k-l+1} - \hat{y}_{k-l+1})^2], \quad (20)$$

where θ_l is an element of the matrix Θ , $\Theta = \{\theta_l\}$, $l \in \mathcal{L}$ defined in (10).

With the auxiliary variable d_y , the auxiliary optimization problem can be formulated as follows,

$$R(D_y) = \inf_{d_y \leq D_y} \frac{1}{L} I(y_{k,1:L}; \hat{y}_{k,1:L}). \quad (21)$$

According to the results in [32], the solution to (21) can be directly obtained:

$$R(D_y) = \frac{1}{2L} h(y_{k,1:L}) - \frac{1}{2} \log 2\pi e D_y + \frac{1}{2} \sum_{l=1}^L \log \theta_l^2. \quad (22)$$

For the aperiodic finite-bits feedback scheme, the MSE between x_{k+1} and its reconstructed version at the base station

can be calculated as follows,

$$\begin{aligned}
d_x^{AP} &= E \left[(x_{k+1} - \hat{x}_{k+1})^2 \right] \\
&= E \left[(x_{k+1} - x'_{k+1} + x'_{k+1} - \hat{x}_{k+1})^2 \right] \\
&= E \left[(x_{k+1} - x'_{k+1})^2 \right] + E \left[(x'_{k+1} - \hat{x}_{k+1})^2 \right] \\
&\quad + 2E \left[(x_{k+1} - x'_{k+1}) (x'_{k+1} - \hat{x}_{k+1}) \right] \\
&\stackrel{(a)}{=} \sigma_P^2 + E \left[\left(\sum_{l=1}^L \theta_l y_{k+1-l} - \sum_{l=1}^L \theta_l \hat{y}_{k+1-l} \right)^2 \right] \quad (23) \\
&\quad + 2E \left[(x_{k+1} - x'_{k+1}) (x'_{k+1} - \hat{x}_{k+1}) \right] \\
&\stackrel{(b)}{=} \sigma_P^2 + E \left[\left(\sum_{l=1}^L \theta_l y_{k+1-l} - \sum_{l=1}^L \theta_l \hat{y}_{k+1-l} \right)^2 \right] \\
&\stackrel{(c)}{=} \sigma_P^2 + \sum_{l=1}^L E \left[\theta_l^2 (y_{k+1-l} - \hat{y}_{k+1-l})^2 \right],
\end{aligned}$$

where (a) follows (13); (b) follows the orthogonal principle, and the quantization noise being an independent and zero mean variable; (c) follows the derivation in the *test* channel shown in [33].

Combining (22) and (23), we obtain the lower bound on the feedback overhead:

$$\begin{aligned}
R(D_x^{AP}) &= \frac{1}{2L} h(y_{k,1:L}) - \frac{1}{2} \log 2\pi e (D_x - \sigma_P^2) + \frac{1}{2} \sum_{l=1}^L \log \theta_l^2 \\
&= h(y_{k,1:L}) - \frac{1}{2} \log 2\pi e (D_x - \sigma_P^2) + \frac{1}{2} \sum_{l=1}^L \log \theta_l^2 \\
&\stackrel{(a)}{=} \log |\mathbf{K}_y| - \frac{1}{2} \log (D_x - \sigma_P^2) + \frac{1}{2} \sum_{l=1}^L \log \theta_l^2 \quad (24)
\end{aligned}$$

where $\mathbf{K}_y = \{\kappa_y(i, j) = \kappa_y(i - j)\}$, and (a) follows

$$\frac{1}{L} h(y_{k,1:L}) = \frac{1}{2} \log 2\pi e + \frac{1}{2L} \log |\mathbf{K}_y| \quad (25)$$

2) *Aperiodic feedback in the zero-holding strategy*: As introduced in the previous section, the ZH assumption is widely adopted in current feedback scheme. Remember that \hat{x}_{k+1}^Z denotes the zero-holding channel state at the $(k+1)$ -th time instance. The estimation of x_k from its noisy observation y_k is taken as the value of \hat{x}_{k+1}^Z , i.e., $\hat{x}_{k+1}^Z = x_k^\dagger = E[x_k | y_k]$.

To calculate the theoretic lower bound on overheads, we define an auxiliary variable d_y^Z which is the weighted MSE between y_k and y_k^\dagger ,

$$d_y^Z = \alpha E \left[(y_k - y_k^\dagger)^2 \right], \quad (26)$$

where $x_k^\dagger = \alpha y_k^\dagger$, and $\alpha = \frac{\sigma_x^2}{\sigma_x^2 + \sigma_\xi^2}$ which is derived from the MMSE estimation of x from its observation y in AWGN.

MSE of the ZH scheme's x_{k+1} and \hat{x}_{k+1}^Z is calculated as

follows,

$$\begin{aligned}
d_x^Z &= E \left[(x_{k+1} - \hat{x}_{k+1}^Z)^2 \right] \\
&= E \left[(x_{k+1} - \alpha y_k + \alpha y_k - \hat{x}_{k+1}^Z)^2 \right] \\
&\stackrel{(a)}{=} E \left[(x_{k+1} - \alpha y_k + \alpha y_k - \alpha y_k^\dagger)^2 \right] \\
&= E \left[(x_{k+1} - \alpha y_k)^2 \right] \\
&\quad + E \left[(\alpha y_k - \alpha y_k^\dagger)^2 \right] \\
&\quad + E \left[(x_{k+1} - \alpha y_k) (\alpha y_k - \alpha y_k^\dagger) \right] \\
&\stackrel{(b)}{=} \sigma_Z^2 + d_y^Z + E[(x_{k+1} - \alpha y_k) (\alpha y_k - \alpha y_k^\dagger)]
\end{aligned} \quad (27)$$

where (a) follows (14), and (b) follows (16) and (26).

Different from the one-step prediction based on multiple previous observations, $y_{k,1:L}$, x_k^\dagger is derived from a single observation y_k in the ZH scheme. We can thus create an auxiliary optimization problem as follows,

$$R(D_y^Z) = \inf_{d_y^Z \leq D_y^Z} I(y_k; y_k^\dagger). \quad (28)$$

The solution to (28) is given as follows,

$$R(D_y^Z) = \frac{1}{2} h(y_k) - \frac{1}{2} \log 2\pi e D_y^Z + \frac{1}{2} \log \alpha. \quad (29)$$

Given (27), we can derive the rate distortion function (29) as follows,

$$\begin{aligned}
R(D_y^Z) &= \frac{1}{2} h(y_k) + \frac{1}{2} \log \left(\frac{\sigma_x^2}{\sigma_x^2 + \sigma_\xi^2} \right) \\
&\quad - \frac{1}{2} \log 2\pi e \left(-E[(x_{k+1} - \alpha y_k) (\alpha y_k - \alpha y_k^\dagger)] \right) \\
&\stackrel{(a)}{=} \frac{1}{2} h(y_k) + \frac{1}{2} \log \left(\frac{\sigma_x^2}{\sigma_x^2 + \sigma_\xi^2} \right) - \frac{1}{2} \log 2\pi e (D_x^Z - \sigma_z^2), \quad (30)
\end{aligned}$$

where (a) is obtained according to the test channel, i.e., $y = \hat{y} + \varkappa$. The test channel is the sufficient and necessary condition in which the equality holds in (28). In the test channel, \varkappa follows the Gaussian distribution with zero mean and variance of D_y^Z . Thus, we have

$$E \left[(x_{k+1} - \alpha y_k) (\alpha y_k - \alpha y_k^\dagger) \right] = 0. \quad (31)$$

The theoretic lower bounds of the two aperiodic channel state feedback schemes have been obtained. The next subsection will investigate the theoretic bounds of the periodic feedback schemes.

B. Periodic Feedback Overhead

Fading channels are usually a stationary random process, which implies that channel states nearby in time domain are correlated to each other. It is thus possible to only transmit different information (i.e., innovation) between samples and reduce the number of feedback bits. Innovation based transmission can be achieved through periodic feedbacks.

In order to calculate the required bits in the periodic feedback, we need to write the noisy observation y with an

autoregressive structure. As shown in (2), a fading channel x is the output of a white Gaussian variable ψ passing through an autoregressive system. At the UE, observed channel states are essentially equal to the summation of x and ξ , shown in (1). Combining (1) and (2), we derive the autoregressive structure of y as follows,

$$\begin{aligned}
y_k &= \sum_{m=1}^L a_m x_{k-m} + \psi_k + \xi_k \\
&\stackrel{(a)}{=} \sum_{m=1}^L a_m \left(\frac{\sigma_x^2}{\sigma_x^2 + \sigma_\xi^2} y_{k-m} + e_{k-m} \right) + \psi_k + \xi_k \\
&= \sum_{m=1}^L a_m \frac{\sigma_x^2}{\sigma_x^2 + \sigma_\xi^2} y_{k-m} + \sum_{m=1}^L a_m e_{k-m} + \psi_k + \xi_k \\
&\stackrel{(b)}{=} \sum_{m=1}^L a_m \frac{\sigma_x^2}{\sigma_x^2 + \sigma_\xi^2} y_{k-m} + \nu_k,
\end{aligned} \tag{32}$$

where e_{k-m} is the difference between an estimated channel state and its real value. e_{k-m} observes zero mean Gaussian distribution with the variance of $\frac{\sigma_x^2 \sigma_\xi^2}{\sigma_x^2 + \sigma_\xi^2}$; (a) follows the MMSE estimation of x under the noise γ ,

$$E[x|y] = \frac{\sigma_x^2}{\sigma_x^2 + \sigma_\xi^2} y \tag{33}$$

(b) follows the definition:

$$\nu_k \triangleq \sum_{m=1}^L a_m e_{k-m} + \psi_k + \xi_k. \tag{34}$$

From the analysis above, y is essentially equal to output of the *i.i.d.* white Gaussian variable ν_k , $\nu_k \sim \mathcal{N}(0, \sigma_\nu^2)$, $\sigma_\nu^2 = \frac{\sigma_x^2 \sigma_\xi^2}{\sigma_x^2 + \sigma_\xi^2} \sum_{m=1}^L a_m^2 + \sigma_\psi^2 + \sigma_\xi^2$, passing through the AR model with the coefficients of $\{\frac{a_m \sigma_x^2}{\sigma_x^2 + \sigma_\xi^2}\}$, $m \in \mathcal{L}$.

According to the results in [34], the rate distortion function with the source of y is equal to the R-D function with the source of ν . Therefore, we derive the lower bound in the periodic feedback scheme as follows,

$$\begin{aligned}
R(D_x) &\stackrel{(a)}{=} \frac{1}{2L} h(y_{k,1:L}) - \frac{1}{2} \log 2\pi e (D_x - \sigma_P^2) + \frac{1}{2} \sum_{l=1}^L \log \theta_l^2 \\
&\stackrel{(b)}{=} \frac{1}{2} \log \frac{\sigma_\nu^2}{D_x - \sigma_P^2} + \frac{1}{2} \sum_{l=1}^L \log \theta_l^2,
\end{aligned} \tag{35}$$

where (a) follows the results shown in [34], (b) follows the same derivation in (24).

In the simulations parts of this paper, we will numerically evaluate and compare the theoretical lower bound on the bit rates for different feedback schemes. Next, we will propose practical channel state feedback schemes, which can be implemented by off-the-shelf signal processing devices or modules.

V. AN PRACTICAL CHANNEL STATE FEEDBACK SCHEME

In the previous section, we calculated the lower bounds on the overhead of the aperiodic and periodic channel state feed-

back schemes. In this section, we propose practical feedback schemes.

A. High Resolution Quantization in Aperiodic Feedback Scheme

In this subsection, we focus on a practical compression method of CSI in the aperiodic scheme. As already pointed out, the compression method of an aperiodical scheme is essentially a scalar quantization process. The sample-wise quantization has been thoroughly studied. Thus, we pay more attention to evaluating the performance of the practical aperiodical feedback schemes.

Due to its most widely usage in current wireless communication systems, uniform quantizers are considered for aperiodic channel state feedback. The MSE between the channel state x_{k+1} and the uniform quantizer output is taken as the metric to measure the feedback distortion. It is worth noting that the input of the quantizer is the predicted channel state \hat{x}_{k+1} .

Let \hat{x}_{k+1}^Q denote the quantized channel state at the $(k+1)$ -th time instance and e_a denote the error between the real channel state and the quantization result. Furthermore, R_a denotes the average number of bits. With the defined variables, we can calculate the MSE as follows,

$$\begin{aligned}
E[e_a^2] &= E \left[\left(x_{k+1} - \hat{x}_{k+1}^Q \right)^2 \right] \\
&= E \left[E \left[\left(x_{k+1} - (\hat{x}_{k+1} + e_a^Q) \right)^2 \middle| e_a^Q \right] \right] \\
&= E \left[E \left[\left(x_{k+1} - \hat{x}_{k+1} \right)^2 \middle| e_a^Q \right] + \left(e_a^Q \right)^2 \right. \\
&\quad \left. + 2E \left[\left(x_{k+1} - \hat{x}_{k+1} \right) e_a^Q \middle| e_a^Q \right] \right] \\
&\stackrel{(a)}{=} E \left[\sigma_P^2 + \left(e_a^Q \right)^2 + 2E \left[\left(x_{k+1} - \hat{x}_{k+1} \right) e_a^Q \middle| e_a^Q \right] \right] \\
&\stackrel{(b)}{=} \sigma_P^2 + E \left[\left(e_a^Q \right)^2 \right] \\
&\stackrel{(c)}{=} \sigma_P^2 + \frac{1}{12} 2^{h(\hat{x})} 2^{-2R_a} \\
&= \sigma_P^2 + \frac{1}{12} \left(2\pi e (\sigma_x^2 + \sigma_P^2) \right)^{\frac{1}{2}} 2^{-2R_a}
\end{aligned} \tag{36}$$

where (a) follows the result in (13), (b) follows that quantization noise e_a^Q is independent to the prediction error $(x_{k+1} - \hat{x}_{k+1})$ and the mean value of quantization noise is zero, (c) is obtained under the assumption of high-resolution uniform quantization.

In (36), the MSE between the reconstructed channel state at BS \hat{x}_{k+1}^Q and x_{k+1} is a function of the number of data bits R_a , which can be denoted as a function of MSE through simple mathematical manipulations,

$$R_a = \frac{1}{2} \log \left(\frac{1}{12} \frac{(2\pi e (\sigma_x^2 + \sigma_P^2))^{\frac{1}{2}}}{E[e_a^2] - \sigma_P^2} \right). \tag{37}$$

B. A Practical Channel State Compression Method in Periodic Feedback Scheme

As shown in Section IV-B, the compressed data of the channel innovation consumes less bits than that for the original channel state. Periodic feedback scheme makes it possible to

employ channel innovation based method. In this subsection, we discuss the details of designing a practical method to compress channel innovation under the impact of fading and additive noise.

Fig. 2 and Fig. 3 describe the structures of the encoder and decoder of the proposed compression scheme. The optimum configurations and performance analysis will be presented to implement the scheme and evaluate its performance.

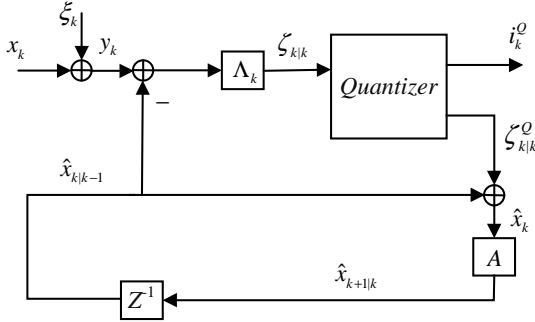


Fig. 2. Encoder of the proposed additive noise degraded channel innovation compression scheme

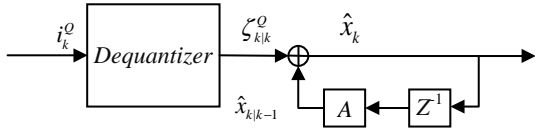


Fig. 3. Decoder of the proposed compression scheme

As shown in Fig. 2, the encoder is built on an innovation compression scheme with a feedback loop. The closed loop compression is designed to avoid quantization noise accumulation. In the compression structure, the innovation is denoted by ζ and its quantization is ζ^Q . The quantized innovation is added to the predicted channel state $\hat{x}_{k|k-1}$ to obtain the estimation of the current channel state \hat{x}_k , where $\hat{x}_{k|k-1}$ is the prediction of the channel state based on the previous L channel states $\hat{x}_{k,1:L}$.

With the reconstructed channel states $\hat{x}_{k+1,1:L} = \{\hat{x}_{k-L+1}, \hat{x}_{k-L+2}, \dots, \hat{x}_k\}$, the channel state at the $(k+1)$ -th time instance is predicted as follows,

$$\hat{x}_{k+1|k} = \sum_{m=1}^L a_m \hat{x}_{k-m+1}. \quad (38)$$

Passing $\hat{x}_{k+1|k}$ through a time delay unit, we have the output $\hat{x}_{k|k-1}$. $\hat{x}_{k|k-1}$ is the estimation of x_k based on $\hat{x}_{k,1:L} = \{\hat{x}_{k-L}, \hat{x}_{k-L+1}, \dots, \hat{x}_{k-1}\}$.

MSE of the prediction, $E[e_{k|k-1}^2]$, where $e_{k|k-1} = x_k - \hat{x}_{k|k-1}$, can be calculated as follows,

$$E[e_{k|k-1}^2] = \sum_{m=1}^L a_m^2 E[e_{k-m}^2] + \sigma_\psi^2 + \sum_{m=1}^L a_m^2 E[e_{k-m}^{Q2}]. \quad (39)$$

Proof: See Appendix A. ■

$\hat{x}_{k|k-1}$ is the initial estimation of x_k . The accuracy in the prediction of x_k is affected by two factors: the estimation error and quantization noise. Therefore, we need to update $\hat{x}_{k|k-1}$

in the closed loop to avoid the accumulation of noise induced by these two factors:

$$\hat{x}_k = \hat{x}_{k|k-1} + \zeta_k^Q, \quad (40)$$

where ζ_k^Q is the quantization output of ζ_k .

Next, we discuss how to obtain ζ_k^Q . The MMSE of the prediction errors with respect to ζ_k^Q is defined as follows

$$\min_{\zeta_k^Q} E[(x_k - \hat{x}_{k|k-1})^2]. \quad (41)$$

Since a fading channel is essentially a time evolution random process, an iterative solution to (41) can be obtained to dynamically approach the optimum value as follows,

$$\zeta_k^Q = E[e_{k|k-1}^2] \left(E[e_{k|k-1}^2] + \sigma_\xi^2 \right)^{-1} (y_k - \hat{x}_{k|k-1}) \quad (42)$$

where $e_{k|k-1} = x_k - \hat{x}_{k|k-1}$.

Proof: See Appendix B. ■

Via the updating method shown in (40), MMSE is asymptotically achieved in an iterative manner. The two mean square errors, $E[e_k^2]$ and $E[e_{k|k-1}^2]$, can thus satisfy the following condition.

$$E[e_k^2] = (1 - \lambda_k) E[e_{k|k-1}^2], \quad (43)$$

where $\lambda_k = E[e_{k|k-1}^2] \left(E[e_{k|k-1}^2] + \sigma_\xi^2 \right)^{-1}$

With the optimum innovation ζ_k^Q , the transmitter can then use the quantization codebook to determine the corresponding index and map it to a symbol for transmission.

At the decoder side, the symbol is first demapped to obtain the codeword index, which is then used to reconstruct the quantized innovation ζ_k^Q . With the reconstructed ζ_k^Q , we can calculate the channel state using the structure presented in Fig. 3. To distinguish from the estimated channel state at the encoder side \hat{x}_k , the reconstructed channel state at the decoder side is denoted by \hat{x}_k^* . As shown in Fig. 3, the reconstructed ζ_k^Q is added to x_k which is the prediction based on the previous L channel states:

$$\hat{x}_k^* = \sum_{m=1}^L a_m \hat{x}_{k-m}^* + \zeta_k^Q. \quad (44)$$

After introducing the the encoder and decoder of the proposed channel state feedback scheme, we will investigate its performance in the next subsection.

C. Performance of the Proposed Feedback Scheme

The same performance metric used in the previous part of this paper: bit-distortion curve is taken to evaluate the performance of the proposed feedback scheme. We first prove that the MSE converges in the long term, and then calculate this long-term MSE, which is defined as follows,

$$\varsigma = \lim_{k \rightarrow \infty} E[(x_k - \hat{x}_k)^2]. \quad (45)$$

Theorem 1 shows that the long-term MSE ς can be expressed in an iterative structure.

Theorem 1. The stable MSE ζ is the solution to the differential equation as follows,

$$\zeta - \left((1 - \lambda)^2 \sum_{m=1}^L a_m^2 \zeta^{(m)} \right) = (1 - \lambda_k)^2 \sigma_\psi^2 + \lambda_k^2 \sigma_\xi^2 + \sigma_Q^2. \quad (46)$$

where $\zeta^{(m)}$ denotes the m -th order derivative of ζ .

Proof: See Appendix C. ■

Let

$$\sum_{m=1}^L f_m e^{c_m n T} \quad (47)$$

and

$$\sum_{m=0}^L g_m (nT)^m \quad (48)$$

denote the general and specific solutions to the differential equation (49). Combining (47) and (48), the solution to (49) is written as follows,

$$\zeta^* = \sum_{m=1}^L f_m e^{c_m n T} + \sum_{m=0}^L g_m (nT)^m. \quad (49)$$

However, it is extremely difficult to obtain the explicit forms of $\{f_m\}$, $\{c_m\}$, and $\{g_m\}$, $m \in \mathcal{L}$. In order to gain insight on the long-term behaviour of MSE ζ , we tackle this problem by introducing the approximation of the channel state process in an order one autoregressive model (AR(1)). Let \tilde{x} denote the approximation of x ,

$$\tilde{x}_k = \beta \tilde{x}_{k-1} + \iota_k. \quad (50)$$

where the coefficient β is determined under the rule of MMSE, that is,

$$\beta = \min_{\beta} E \left[(x_k - \beta \tilde{x}_{k-1})^2 \right], \quad (51)$$

and ι is a zero mean Gaussian random process with the variance of σ_ι^2 to be determined.

From (51), we obtain the value of β as follows,

$$\beta = \frac{\kappa_x(1)}{\kappa_x(0)}. \quad (52)$$

With the calculated β , the variance σ_ι^2 is correspondingly determined,

$$\sigma_\iota^2 = \kappa_x(0) - \frac{\kappa_x^2(1)}{\kappa_x(0)}. \quad (53)$$

Afterwards, we calculate the MSE of the approximated solution. Following a similar method as (46), we obtain a first order differential equation as follows,

$$\tilde{\zeta}_k - (1 - \lambda_k)^2 \beta^2 \tilde{\zeta}_{k-1} = (1 - \lambda_k)^2 \sigma_\iota^2 + \lambda_k^2 \sigma_\xi^2 + \sigma_Q^2. \quad (54)$$

From (54), the long-term value of $\tilde{\zeta}$ can be calculated as

follows,

$$\tilde{\zeta}_\infty = \lim_{K \rightarrow \infty} \left(\frac{\left((1 - \lambda_k)^2 \beta^2 \right)^K \tilde{\zeta}_0}{\left((1 - \lambda_k)^2 \sigma_\iota^2 + \lambda_k^2 \sigma_\xi^2 + \sigma_Q^2 \right) \times \frac{1 - \left((1 - \lambda_k)^2 \beta^2 \right)^K}{1 - (1 - \lambda_k)^2 \beta^2}} \right) \quad (55)$$

$$\stackrel{(a)}{=} \frac{(1 - \lambda_k)^2 \sigma_\iota^2 + \lambda_k^2 \sigma_\xi^2 + \sigma_Q^2}{1 - (1 - \lambda_k)^2 \beta^2},$$

where (a) follows $0 < (1 - \lambda_k) < 1$ and $0 < \beta < 1$.

After calculating the long-term MSE, we investigate the quantization bits in our analysis to obtain the bit versus MSE curve. In the proposed feedback scheme, the quantization objective is essentially equal to the prediction error e_P , i.e., $e_P = x_k - E[x_k | y_k - 1]$. Thus, the statistic feature of e_P is a function of the quantization bit number. However, we can hardly calculate the explicit distribution function of e_P . As an extreme case, when e_P follows a Gaussian distribution, the quantization of e_P requires the largest number of bits in order to meet the same level of errors. We can assume the quantization objective follows the zero mean Gaussian distribution.

To estimate the bit number, we calculate the variance of e_P under the Gaussian distribution assumption. The calculation of $E[e_P^2]$ is derived as follows,

$$\begin{aligned} E[e_P^2] &= \kappa_{\tilde{x}}(0) - \frac{\kappa_{xy}^2(1)}{\kappa_{xy}(0) + \sigma_\xi^2} \\ &= \kappa_{\tilde{x}}(0) - \frac{\kappa_x^2(1)}{\kappa_x(0) + \sigma_\xi^2}. \end{aligned} \quad (56)$$

where

$$\kappa_{\tilde{x}}(0) = \int_{-\pi}^{\pi} \left(\kappa_x(0) - \frac{\kappa_x^2(1)}{\kappa_x(0)} \right) \frac{1}{|1 - \beta e^{j\omega}|^2} d\omega. \quad (57)$$

$$\begin{aligned} \kappa_{\tilde{x}}(1) &= \beta \int_{-\pi}^{\pi} \left(\kappa_x(0) - \frac{\kappa_x^2(1)}{\kappa_x(0)} \right) \frac{1}{|1 - \beta e^{j\omega}|^2} d\omega \\ &= \int_{-\pi}^{\pi} \left(\kappa_x(1) - \frac{\kappa_x^3(1)}{\kappa_x^2(0)} \right) \frac{1}{|1 - \beta e^{j\omega}|^2} d\omega. \end{aligned} \quad (58)$$

Next, we aim to work out the relationship between the number of quantization bits and the quantization error. In uniform quantization, the mean square of the quantization error is denoted by $\sigma_{Q_u}^2$. Let R_u denote the average number of bits for quantization. Under the high resolution quantization assumption, R_u and $\sigma_{Q_u}^2$ satisfy the following equation,

$$\begin{aligned} \sigma_{Q_u}^2 &\stackrel{(a)}{\cong} \frac{1}{12} 2^{h(e_P)} 2^{-2R_u} \\ &= \frac{1}{12} 2^{\frac{1}{2} \log 2\pi e E[e_P^2]} 2^{-2R_u}, \end{aligned} \quad (59)$$

Substituting the corresponding parts of (60) with (55) and

(56), we have

$$R_u = \frac{1}{2} \log \frac{1}{12} + \frac{1}{2} \log \sqrt{2\pi e \kappa_{\bar{x}}(0) - \frac{\kappa_{\bar{x}}^2(1)}{\kappa_{\bar{x}}(0) + \sigma_{\xi}^2}} - \frac{1}{2} \log \left((1 - (1 - \lambda_k)^2 \beta^2) \tilde{\zeta}_{\infty} - (1 - \lambda_k)^2 \sigma_l^2 + \lambda_k^2 \sigma_{\xi}^2 \right). \quad (60)$$

From (60), we can easily know the average number of bits R_u at a given prediction MSE $\tilde{\zeta}_{\infty}$, or the inverse relation between $\tilde{\zeta}_{\infty}$ and R_u .

VI. NUMERICAL SIMULATIONS

In this section, we first numerically study the theoretical lower bounds of different feedback schemes. Afterwards, extensive numerical simulations have been performed to evaluate the proposed practical feedback method. In the simulation, we consider a more practical fading channel, which is the output of an AR(4) model with a white Gaussian random variable. The same assumption that the channel x cannot not be directly observable at the receiver due to the AWGN ξ is introduced. Therefore, four previous noisy channel observations are exploited to predict the one-step ahead channel state.

The traditional ZH method is also simulated in order to provide performance comparison. Furthermore, the theoretical lower bounds for both aperiodical and periodical feedback schemes are studied. As discussed in the previous sections, in the aperiodical scheme, the original channel states are quantized for feedback, while in the periodical one, channel innovations are quantized and sent back to the base station.

First, we calculate the bit rate R versus channel distortion D for all the three schemes: *zero-holding*, *prediction+aperiodical*, and *prediction+periodical*. The R-D curves are generated by varying the input variance of the AR model. Fig. 4 shows the results.

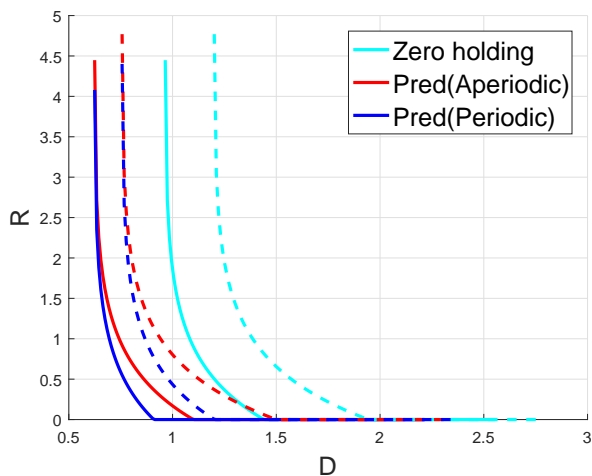


Fig. 4. Bit rate versus channel distortion under varied input variances to the channel AR model.

In Fig. 4, the solid lines are the results with $\sigma_{\psi}^2 = 1$. Remember that ψ is the white Gaussian variable which is the

input to the AR model to generate the fading channel. The dashed lines correspond to $\sigma_{\psi}^2 = 2$.

From Fig. 4, we can observe that the number of bits decreases with the increase of channel state reconstruction error. Furthermore, there is a bound on the distortion in curve, that is, the reconstruction error can not be smaller than a threshold value even if the number of bits is infinitely large. This bound is determined by the finite channel prediction accuracy which is irrelevant to the channel state feedback bits.

The ZH feedback scheme requires more bits at the same distortion level compared with the proposed schemes. This disadvantage is caused by the lower prediction accuracy since it simply takes the channel state at the current time instance for the next time stance. Furthermore, among *aperiodical + prediction* and *periodical + prediction*, the latter requires less bits since only innovations between consecutive channel states are transmitted and the innovations usually have smaller entropy than the original channel samples. It is worth noting that the two curves overlap with each other when the number of bits becomes sufficiently large. In the extreme case of infinite bits quantization, no channel information loss will be caused by the quantization, therefore, the distortion is purely determined by the prediction error.

Furthermore, from Fig. 4, all curves shift right when the channel variance increases. The reason is that increased variance raises the channel entropy, thus more bits are needed at the same distortion level.

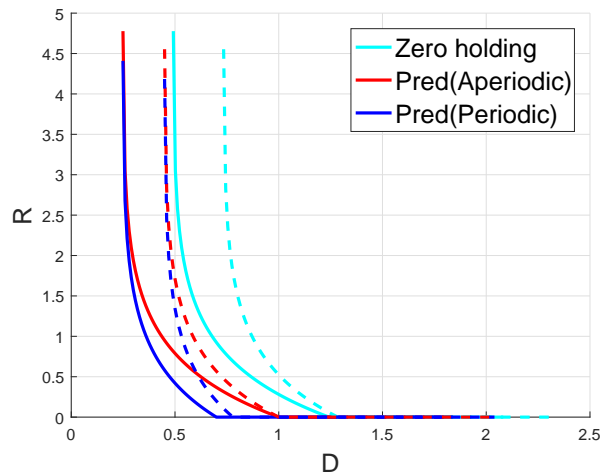


Fig. 5. Bit rate versus distortion under varied additive Gaussian noise

Fig. 5 presents the R-D curves where the variance of the channel model is fixed, while the strength of the additive noise varies. Generally, the number of bits decreases with the increase of noise strength. The ZH scheme generates the largest distortion at the same noise level, compared with the other two schemes. All curves have bounds on distortion when the number of bits increases to the infinity. The *prediction + aperiodical* and *prediction+periodical* schemes have the same bounds.

The major difference between Fig. 5 and Fig. 4 lies in the two curves of the *prediction + aperiodical* scheme. For dif-

ferent level of additive Gaussian noise, the bit rate approaches to zero at the same value of distortion. When no bit is used to transmit the channel states, the distortion is purely determined by the variance of the channel. Since the two curves with different levels of noise have the same channel variance, the distortion at zero bit rate is the same. However, the variance of channel innovations is related to the additive noise. Therefore, the R-D curves of the *prediction+aperiodical* scheme have different zero-bits distortions if the additive noise is not the same.

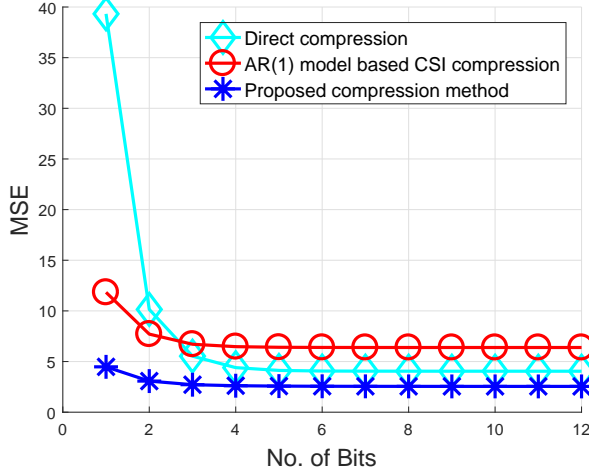


Fig. 6. Number of bits versus channel reconstruction MSE in the proposed CSI feedback schemes

In order to investigate the performance of the proposed CSI feedback scheme, we calculate the curves of the channel reconstruction MSE versus the number of feedback bits. The experiment results are plotted in Fig. 6 for the following three schemes: 1) the channel state is directly quantized and sent back to the base station. This method is widely applied in current systems; 2) the channel is modeled as an AR(1) model without considering additive noise. Under such model, the innovation between two consecutive channel states is quantized and sent back to the base station; 3) a more practical scheme with a high-order AR model under AWGN. The compression method proposed in Section V-B is used for transmitting CSI.

Fig. 6 shows that, the direct quantization scheme generates the largest channel reconstruction MSE when the number of bits is small. If the feedback bits increases, the reconstruction MSE decreases and reaches a stable level that is lower than the AR(1) model. The direct quantization scheme's MSE is determined by the additive noise imposed on the fading channel. The MSE of the AR(1) model is always larger than the proposed method, which is caused by the following two factors: first, the AR(1) model is not accurate and introduces some error when expressing a fading channel; second, the additive Gaussian noise is not considered and adds to the quantization error.

VII. CONCLUSIONS

In this paper, we investigate the overhead introduced by CSI feedback both theoretically and practically, under the periodical and aperiodical CSI feedback schemes that are employed by the LTE standard and discussed in designing future 5G systems. Within these two schemes, we calculate the theoretical lower bounds on the bits for conveying channel states. We observe that the bound of the periodical feedback scheme is lower than the aperiodical scheme, because the channel innovation feedback removes the redundancy so that less bits are needed. We also consider a more practical channel model than the AR(1) model widely accepted in current research on CSI feedback, as well as the additive noise that deteriorates channel states, and propose a practical CSI feedback scheme, which periodically sends the channel state innovation estimated from the noisy observation of channel states in a highly efficient and effective manner. Simulations show that the proposed CSI feedback scheme outperforms those in literature, and suggest its potentially significant contribution to the future generation of wireless communication systems.

APPENDIX

A. Proof of equation (39)

Proof: The error in the prediction of x_k based on $\mathbf{x}_{k-L:L}$ where $\mathbf{x}_{k-L:L} = [x_{k-L}, x_{k-L+1}, \dots, x_{k-1}]$ is defined as follows,

$$\begin{aligned} e_{k|k-1} &= x_k - \hat{x}'_{k|k-1} \\ &= \mathbf{a}^T \mathbf{x}_{k-L:L} + \psi_k - \mathbf{a}^T \hat{\mathbf{x}}_{k-L:L} - \mathbf{a}^T \mathbf{e}_{k-L:L}^Q \\ &= \mathbf{a}^T \mathbf{e}_{k-L:L} + \psi_k - \mathbf{a}^T \mathbf{e}_{k-L:L}^Q, \end{aligned} \quad (61)$$

where

$$\begin{aligned} \mathbf{a} &= [a_1, a_2, \dots, a_L]^T \\ \hat{\mathbf{x}}_{k-L:L}^T &= [\hat{x}_{k-L}, \hat{x}_{k-L+1}, \dots, \hat{x}_{k-1}]^T \\ \mathbf{e}_{k-L:L}^Q &= [e_{k-L}^Q, e_{k-L+1}^Q, \dots, e_{k-1}^Q]^T \\ \mathbf{e}_{k-L:L} &= [e_{k-L}, e_{k-L+1}, \dots, e_{k-1}]^T. \end{aligned} \quad (62)$$

Therefore, the mean square error in the prediction of x_k based on the L past observations is calculated as follows,

$$\begin{aligned} E[e_{k|k-1}^2] &= E[e_{k|k-1} e_{k|k-1}^H] \\ &= E\left[\left(\mathbf{a}^T \mathbf{e}_{k-L:L} + \psi_k - \mathbf{a}^T \mathbf{e}_{k-L:L}^Q\right) \cdot \left(\mathbf{a}^T \mathbf{e}_{k-L:L} + \psi_k - \mathbf{a}^T \mathbf{e}_{k-L:L}^Q\right)^H\right] \\ &\stackrel{(a)}{=} E\left[\mathbf{a}^T \mathbf{e}_{k-L:L} \mathbf{e}_{k-L:L}^H \mathbf{a}\right] + E\left[\psi_k^2\right] \\ &\quad + E\left[\mathbf{a}^T \mathbf{e}_{k-L:L}^Q \mathbf{e}_{k-L:L}^Q H_{k-L:L} \mathbf{a}\right] \\ &\stackrel{(b)}{=} E\left[\mathbf{a}^T \text{diag}\{e_{k-L}^2, e_{k-L+1}^2, \dots, e_{k-1}^2\} \mathbf{a}\right] + E\left[\psi_k^2\right] \\ &\quad + E\left[\mathbf{a}^T \text{diag}\{e_{k-L}^{Q^2}, e_{k-L+1}^{Q^2}, \dots, e_{k-1}^{Q^2}\} \mathbf{a}\right] \\ &= \sum_{m=1}^L b_m^2 e_{k-m}^2 + \sigma_\psi^2 + \sum_{m=1}^L b_m^2 e_{k-m}^{Q^2} \end{aligned} \quad (63)$$

where (a) follows that the estimation error e is independent to both the additive noise ψ and the quantization noise e^Q , and

the quantization noise e^Q is independent to ψ ; (b) follows that

$$E[e_{k_1} e_{k_2}] = \begin{cases} e_{k_1}^2, & k_1 = k_2 \\ 0, & k_1 \neq k_2 \end{cases}$$

and

$$E[e_{k_1}^Q e_{k_2}^Q] = \begin{cases} \sigma_Q^2, & k_1 = k_2 \\ 0, & k_1 \neq k_2 \end{cases}.$$

Thus, the proof is completed. \blacksquare

B. Proof of equation (40)

Proof:

In the iterative calculation for the optimum updating, the noisy channel state y_k is the only variable which can be observed. The noisy observation is taken to assist the optimum updating. Thus, we first write the difference between the predicted noisy observation and the real observation y_k , which is also called as the innovation, as follows,

$$\mu_k = y_k - \hat{x}_{k|k-1}. \quad (64)$$

The calculated μ_k is essentially observed value which is not optimized. To achieve the updating in rule of MMSE, an modification on μ_k is needed. We consider the multiplicative factor to modify μ_k such that the MMSE updating can be achieved. In the second step, we thus calculate the product between the gain λ_k and μ_k as follows,

$$\zeta_k = \lambda_k \mu_k, \quad (65)$$

where λ_k is denotes the gain.

The quantized ζ_k , denoted by ζ_k^Q , is used in the MMSE updating. Thus, the quantized innovation ζ_k^Q is used in the following calculation of MSE. In the quantization of ζ_k , we consider uniform quantization due to its most widely use. The mean square error of x_k with respect to \hat{x}_k is calculated as follows,

$$\begin{aligned} E[e_k^2] &= E[e_k e_k^H] \\ &= E\left[(x_k - \hat{x}_k)(x_k - \hat{x}_k)^H\right] \\ &\stackrel{(a)}{=} E\left[\left(x_k + \xi_k - \hat{x}'_{k|k-1} - \lambda_k(y_k - \hat{x}_{k|k-1}) - e_k^Q\right) \cdot \left(x_k + \xi_k - \hat{x}_{k|k-1} - \lambda_k(x_k + \xi_k - \hat{x}_{k|k-1}) - e_k^Q\right)^H\right] \\ &\stackrel{(b)}{=} E\left[(1 - \lambda_k)(x_k - \hat{x}_{k|k-1})(x_k - \hat{x}_{k|k-1})^H (1 - \lambda_k)^H + \lambda_k \xi_k \xi_k^H \lambda_k^H + e_k^Q (e_k^Q)^H\right] \\ &= E\left[(1 - \lambda_k) e_{k|k-1}^2 (1 - \lambda_k)^H + \lambda_k \sigma_\xi^2 \lambda_k^H + \sigma_Q^2\right], \end{aligned} \quad (66)$$

where (a) follows (1), (64), (65), and (40); ζ_k^Q is the error in quantizing ζ_k . (b) follows the fact that the additive noise ξ is independent to all of three terms: the channel state x , the prediction of x based on their observations in past time instances, and the quantization noise e^Q ; furthermore, (b) is obtained according to the weak assumption that the quantization noise is independent to the channel state x and its linear estimation.

Next, we calculate the derivative of $E[e_k^2]$ with respect to λ_k and calculate the λ_k generating the zero derivative,

$$\frac{dE[e_k^2]}{d\lambda_k} = 0. \quad (67)$$

After solving (67), we have the optimum gain shown as follows,

$$\lambda_k^* = E[e_{k|k-1}^2] \left(E[e_{k|k-1}^2] + \sigma_\xi^2\right)^{-1} \quad (68)$$

where $E[e_{k|k-1}^2]$ denotes the mean square error matrix calculated in the previous round of compression.

After combining (64), (65), and (68), the proof is completed. \blacksquare

C. Proof of Theorem 1

Before calculating ς_k , we rewrite \hat{x}_k into an iterative structure. Combining (40), (43), (65) and (64), we have the reconstruction of channel state at k -th time instance,

$$\begin{aligned} \hat{x}_k &= \hat{x}_{k|k-1} + \lambda_k \left(y_k - \hat{x}_{k|k-1}\right) + e_k^Q \\ &= \sum_{m=1}^L a_m \hat{x}_{k-m} \\ &\quad + \lambda_k \left(\sum_{m=1}^L a_m (x_{k-m} - \hat{x}_{k-m}) + \psi_k + \xi_k\right) + e_k^Q, \end{aligned} \quad (69)$$

where e_k^Q denotes the quantization noise.

Afterwards, we calculate the long-term reconstruction MSE at k -th time instance and write it into an iterative structure. The derivations are as follow

$$\begin{aligned} \varsigma_k &= E\left[(x_k - \hat{x}_k)^2\right] \\ &= E\left[\left(\sum_{m=1}^L a_m x_{k-m} + \psi_k - \sum_{m=1}^L a_m \hat{x}_{k-m} - \lambda_k \left(\sum_{m=1}^L a_m (x_{k-m} - \hat{x}_{k-m}) + \psi_k + \xi_k\right) - e_k^Q\right)^2\right] \\ &\stackrel{(a)}{=} (1 - \lambda_k)^2 E\left[\left(\sum_{m=1}^L a_m (x_{k-m} - \hat{x}_{k-m})\right)^2\right] \\ &\quad + (1 - \lambda_k)^2 \sigma_\psi^2 + \lambda_k^2 \sigma_\xi^2 + \sigma_Q^2 \\ &\stackrel{(b)}{=} (1 - \lambda_k)^2 E\left[\left(\sum_{m=1}^L a_m^2 (x_{k-m} - \hat{x}_{k-m})^2\right)\right] \\ &\quad + (1 - \lambda_k)^2 \sigma_\psi^2 + \lambda_k^2 \sigma_\xi^2 + \sigma_Q^2 \\ &= (1 - \lambda_k)^2 E\left[\left(\sum_{m=1}^L a_m^2 \varsigma_{k-m}\right)\right] \\ &\quad + (1 - \lambda_k)^2 \sigma_\psi^2 + \lambda_k^2 \sigma_\xi^2 + \sigma_Q^2 \end{aligned} \quad (70)$$

where (a) follows the facts, ψ , ξ , and e^Q are independent to each other; ψ_{k_1} is uncorrelated with the channel states x_{k_2} and noisy channel observations y_{k_2} before the k_1 -th time instance, $k_1 > k_2$; Similarly, ξ_{k_1} is also uncorrelated with the channel states x_{k_2} and noisy channel observations y_{k_2} for $k_1 > k_2$;

(b) follows the equation below

$$\begin{aligned} & E \left[\left(\sum_{m=1}^L a_m (x_{k-m} - \hat{x}_{k-m}) \right)^2 \right] \\ &= E \left[\left(\sum_{m=1}^L a_m^2 (x_{k-m} - \hat{x}_{k-m})^2 \right) \right]. \end{aligned} \quad (71)$$

which follows the result in Lemma 1.

From (70), we build a differential equal shown in Theorem 1.

Thus, the proof is completed.

Lemma 1. *Cross terms in the mean square error between linear combinations are approximately equal to zero*

$$E[(x_{k_1} - \hat{x}_{k_1})(x_{k_2} - \hat{x}_{k_2})] = 0, \quad (72)$$

where $k_1 \neq k_2$.

Proof: According to the derivation of (67), the \hat{x} is a minimum mean square error estimation of x based on its noisy observation y . According to the orthogonal principle, the estimation error $(x - \hat{x})$ is orthogonal to y . Furthermore, \hat{x} is a linear combination of y . Thus, $(x - \hat{x})$ is also orthogonal to \hat{x} , that is,

$$E[(x - \hat{x})\hat{x}] = 0. \quad (73)$$

We can straightforwardly prove the mean of the estimation error is zero. Furthermore, via a numeric method, we can show the estimation error at a time instance, say k_1 , is independent to the channel state at a different time instance, say k_2 , $k_1 \neq k_2$. Therefore, we have

$$E[(x_{k_1} - \hat{x}_{k_1})\hat{x}_{k_2}] = E[(x_{k_1} - \hat{x}_{k_1})]E[\hat{x}_{k_2}] = 0. \quad (74)$$

According to the results in (73) and (74), the cross terms in $E \left[\left(\sum_{m=1}^L a_m (x_{k-m} - \hat{x}_{k-m}) \right)^2 \right]$ are equal to zero. Thus, the proof of the Lemma is completed. ■

REFERENCES

- [1] P. Huang and D. Rajan, "Estimation of centralized spectrum sensing overhead for cognitive radio networks," in *2014 IEEE 25th Annual International Symposium on Personal, Indoor, and Mobile Radio Communications (PIMRC)*, Sept 2014, pp. 659–663.
- [2] P. Huang and Y. Pi, "Wireless internet assisting satellite position in urban environments," in *2011 6th International ICST Conference on Communications and Networking in China (CHINACOM)*, Aug 2011, pp. 262–267.
- [3] —, "Urban environment solutions to gps signal near-far effect," *IEEE Aerospace And Electronic Systems Magazine*, vol. 26, no. 5, pp. 18–27, 2011.
- [4] P. Huang, Y. Pi, and I. Progi, "Gps signal detection under multiplicative and additive noise," *Journal of Navigation*, vol. 66, no. 04, pp. 479–500, 2013.
- [5] T. R. Lakshmana, A. Tlli, R. Devassy, and T. Svensson, "Precoder design with incomplete feedback for joint transmission," *IEEE Transactions on Wireless Communications*, vol. 15, no. 3, pp. 1923–1936, March 2016.
- [6] K. Anand, E. Gunawan, and Y. L. Guan, "Precoder designs for the relay-aided x channel without source csi," *IEEE Transactions on Signal Processing*, vol. 65, no. 1, pp. 41–55, Jan 2017.
- [7] H. Wang, R. Song, and S. H. Leung, "Throughput analysis of interference alignment for a general centralized limited feedback model," *IEEE Transactions on Vehicular Technology*, vol. 65, no. 10, pp. 8775–8781, Oct 2016.
- [8] M. Rezaee and M. Guillaud, "Interference alignment with quantized grassmannian feedback in the k-user constant mimo interference channel," *IEEE Transactions on Wireless Communications*, vol. 15, no. 2, pp. 1456–1468, Feb 2016.
- [9] M. R. Abedi, N. Mokari, M. R. Javan, and H. Yanikomeroglu, "Limited rate feedback scheme for resource allocation in secure relay-assisted ofdma networks," *IEEE Transactions on Wireless Communications*, vol. 15, no. 4, pp. 2604–2618, April 2016.
- [10] M. Javan, N. Mokari, F. Alavi, and A. Rahmati, "Resource allocation in decode-and-forward cooperative communications networks with limited rate feedback channel," *IEEE Transactions on Vehicular Technology*, vol. PP, no. 99, pp. 1–1, 2016.
- [11] X. Yang and A. L. Swindlehurst, "Limited rate feedback in a mimo wiretap channel with a cooperative jammer," *IEEE Transactions on Signal Processing*, vol. 64, no. 18, pp. 4695–4706, Sept 2016.
- [12] L. Wang, Y. Cai, Y. Zou, W. Yang, and L. Hanzo, "Joint relay and jammer selection improves the physical layer security in the face of csi feedback delays," *IEEE Transactions on Vehicular Technology*, vol. 65, no. 8, pp. 6259–6274, Aug 2016.
- [13] M. E. Eltayeb, T. Y. Al-Naffouri, and H. R. Bahrami, "Compressive sensing for feedback reduction in mimo broadcast channels," *IEEE Transactions on Communications*, vol. 62, no. 9, pp. 3209–3222, Sept 2014.
- [14] Z. Lv and Y. Li, "A channel state information feedback algorithm for massive mimo systems," *IEEE Communications Letters*, vol. 20, no. 7, pp. 1461–1464, July 2016.
- [15] P. H. Kuo, H. T. Kung, and P. A. Ting, "Compressive sensing based channel feedback protocols for spatially-correlated massive antenna arrays," in *2012 IEEE Wireless Communications and Networking Conference (WCNC)*, April 2012, pp. 492–497.
- [16] P. Huang, M. Tonnemacher, Y. Du, D. Rajan, and J. Camp, "Towards scalable network emulation: Channel accuracy versus implementation resources," in *INFOCOM, 2013 Proceedings IEEE*, April 2013, pp. 1959–1967.
- [17] P. Huang, D. Rajan, and J. Camp, "Weibull and suzuki fading channel generator design to reduce hardware resources," in *Wireless Communications and Networking Conference (WCNC), 2013 IEEE*, April 2013, pp. 3443–3448.
- [18] P. Huang, Y. Du, and Y. Li, "Stability analysis and hardware resource optimization in channel emulator design," *IEEE Transactions on Circuits and Systems I: Regular Papers*, vol. 63, no. 7, pp. 1089–1100, July 2016.
- [19] P. Huang, D. Rajan, and J. Camp, "An autoregressive doppler spread estimator for fading channels," *IEEE Wireless Communications Letters*, vol. 2, no. 6, pp. 655–658, 2013.
- [20] M. Zhou, L. Zhang, L. Song, and M. Debbah, "A differential feedback scheme exploiting the temporal and spectral correlation," *IEEE Transactions on Vehicular Technology*, vol. 62, no. 9, pp. 4701–4707, Nov 2013.
- [21] Y. S. Jeon, H. M. Kim, Y. S. Cho, and G. H. Im, "Time-domain differential feedback for massive miso-ofdm systems in correlated channels," *IEEE Transactions on Communications*, vol. 64, no. 2, pp. 630–642, Feb 2016.
- [22] K. Kim, T. Kim, D. J. Love, and I. H. Kim, "Differential feedback in codebook-based multiuser mimo systems in slowly varying channels," *IEEE Transactions on Communications*, vol. 60, no. 2, pp. 578–588, February 2012.

- [23] L. Zhang, L. Song, M. Ma, and B. Jiao, "On the minimum differential feedback for time-correlated mimo rayleigh block-fading channels," *IEEE Transactions on Communications*, vol. 60, no. 2, pp. 411–420, February 2012.
- [24] I. Nevat, G. W. Peters, K. Avnit, F. Septier, and L. Clavier, "Location of things: Geospatial tagging for iot using time-of-arrival," *IEEE Transactions on Signal and Information Processing over Networks*, vol. 2, no. 2, pp. 174–185, June 2016.
- [25] J. Szurley, A. Bertrand, and M. Moonen, "Topology-independent distributed adaptive node-specific signal estimation in wireless sensor networks," *IEEE Transactions on Signal and Information Processing over Networks*, vol. 3, no. 1, pp. 130–144, March 2017.
- [26] W. Jake, *Microwave Mobile Communication*. Piscataway, NJ: Wiley-IEEE Press, 1974.
- [27] P. Huang, W. Wang, and Y. Pi, "Estimation on channel state feedback overhead lower bound with consideration in compression scheme and feedback period," *IEEE Transactions on Communications*, vol. 65, no. 3, pp. 1219–1233, March 2017.
- [28] P. Huang and D. Rajan, "Bounds on the overhead of spectrum sensing in cognitive radio," in *2014 IEEE Global Communications Conference*, Dec 2014, pp. 846–850.
- [29] P. Huang and Y. Pi, "An improved location service scheme in urban environments with the combination of GPS and mobile stations," *Wireless Communications and Mobile Computing*, vol. 14, no. 13, pp. 1287–1301, 2014. [Online]. Available: <http://dx.doi.org/10.1002/wcm.2232>
- [30] P. Huang, "Study on a low complexity ecg compression scheme with multiple sensors," *arXiv preprint arXiv:1704.01612*, 2017.
- [31] A. H. Sayed, *Fundamentals of Adaptive Filtering*. New York, NY, USA: Wiley, 2003.
- [32] T. Berger, *Rate Distortion Theory and Data Compression*. Vienna: Springer Vienna, 1975, pp. 1–39.
- [33] —, *Rate Distortion Theory: A Mathematical Basis for Data Compression*, ser. Prentice-Hall electrical engineering series. Prentice-Hall, 1971. [Online]. Available: <https://books.google.com/books?id=-HV1QgAACAAJ>
- [34] R. Zamir, Y. Kochman, and U. Erez, *IEEE Transactions on Information Theory*, no. 7, pp. 3354–3364, July.

